

Original Article

Copper Based *N,N*-Dimethyl-*N*-(1-Pyridinylmethylidene) Propane-1,3-Diamine Compound: Synthesis, Characterization, and Its Application toward Biocidal Activity



Rajesh Kumar Das* | Deboshmita Mukherjee | Sahin Reja | Kaushik Sarkar | Ambica Kejriwal

Department of Chemistry, University of North Bengal, Bengal, India

Use your device to scan and read the article online



Citation R.K. Das, D. Mukherjee, S. Reja, K. Sarkar, A. Kejriwal. **Copper Based *N,N*-Dimethyl-*N*-(1-Pyridinylmethylidene) Propane-1,3-Diamine Compound: Synthesis, Characterization, and Its Application toward Biocidal Activity.** *J. Appl. Organomet. Chem.*, 2023, 3(2), 73-85.

doi <https://doi.org/10.22034/JAOC.2023.382873.1067>



Article info:

Received: 23 January 2023
Accepted: 17 March 2023
Available Online: 25 March 2023
ID: JAOC-2301-1067
Checked for Plagiarism: Yes

Keywords:

DPMPD, CDMPD, Anticancer activity, DFT, Docking

ABSTRACT

The N3 tridentate ligand *N,N*-dimethyl-*N*-(1-pyridinylmethylidene) propane-1,3-diamine (DPMPD) and its copper complex (CDPMPD) were synthesized of which metal complex is found in green colour powdered form. The associated spectroscopic techniques were used to characterize both ligand and the metal complex. Powder XRD method was utilized using the Scherrer formula to accomplish the grain size of the metal complex. It was found that the experimental results of the powdered complex were quite similar to that of the reference material with JCPDS ID 00- 024-1977. *In vitro* anticancer activity shows that the metal complex exhibits a moderate cytotoxic effect on Hep-G2 cell line. This cytotoxic phenomenon is well supported by a molecular docking study using target topoisomerase II crystal structure (PDB id 4FM9). The HOMO- LUMO energy gap, predicted from the DFT study, signifies that the complex is susceptible to chemically reactive.

Introduction

The DNA structure can lead a chemist towards the synthesis of a new drug molecule to prevent bacteria, viruses, and even cancer. Investigation of nucleic acid analogues is one of the approaches that have been intensively explored [1-2]. The basic structure of a nucleic acid fragment consists of a heterocyclic nitrogenous base (purine or pyrimidine) along with sugar [3].

Most of the pharmaceuticals compounds [4] are heterocyclic and widely used as agrochemicals and as veterinary products owing to their extensive chemical reactivity. Besides, they are further found as sensitizers, developers, antioxidants, corrosion inhibitors, copolymers, and dyestuff [5].

Pyridine, pyrrole, furan, and thiophene are the eminent and the simplest heterocyclic compounds. Among all the heterocyclic

*Corresponding Author: Rajesh Kumar Das (rajeshnbu@gmail.com)

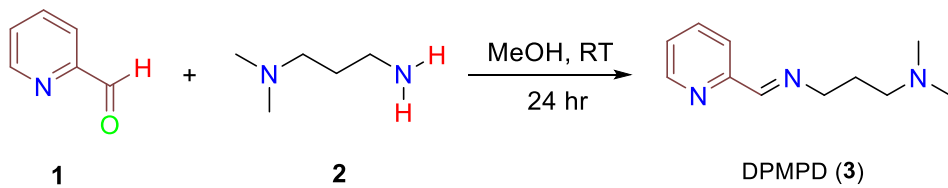
compounds, pyridine derivatives are exceptionally important in pharmaceuticals as well as in bioactive natural products. In the US, pyridine is the main scaffold in most FDA approved medicines [6].

According to the History of pyridine, picoline, the first pyridine base was isolated in 1846 by Anderson from coal-tar and after years of effort, he isolated lutidine and pyridine from a bone oil fraction [7]. Although it required quite a long time to determine its structure by Wilhelm Körner in 1869 and James Dewar in 1871 independently. William Ramsay synthesized the initial hetero-aromatic compound pyridine in 1876 by combining acetylene and hydrogen cyanide [7]. One of the very famous drugs used for the treatment of dermatitis and dementia i.e. niacin [8] in the 1930s, also contains pyridine moiety.

The enriched historical background of pyridine in both the pharmaceutical and agrochemical industry was intended to choose pyridine derivative as the starting point of our synthesis. Very recently Wu-Bin Zhang *et al.* in their journal [9] highlighted the importance of pyridine scaffold as versatile building blocks in organic synthesis and ligand design. They have also shown some examples of pyridine ring being utilised in pharmaceuticals as well as in natural products. E. Lukevits in his article listed several drugs *e.g.*, Nialamide, an Antidepressant, Niaprazine, Sedative; Bromazepam, Tranquilizer and many more and interestingly all of them are pyridine derivatives. Thigulla *et al.* have been synthesized [10] fused chromeno[4,3-b]pyrrolo [3,2-h]quinolin-7(1H)-one and found the anticancer activity of the prepared

compounds [9,10]. Ashraf H. Abadi along with his co-workers synthesised a variety of new compounds containing pyridine derivatives that performed well as anticancer agents [11]. Utilising the bioactivity of pyridine, M.H. Helal and his team synthesized a few compounds that show anticancer activity along with antitumor, anti-inflammatory, and analgesic activities [12]. All these sources suggest that choosing a pyridine derivative for our synthesis would be beneficial in terms of cytotoxic effect.

A number of pyridine-derived ligands have been shown to be antitumor agents, with the resulting complexes exhibiting high cytotoxicity when bound to metals. Among the first transition metals, Cu (II) complexes have shown promising activities. The study of copper (II) complexes of Schiff bases with nitrogen-donating ligands has recently been of interest to researchers not only for their diverse structural features, but also for their potential applications in various fields. Utilising the pyridine bioactivity, M.H. Helal and his team synthesised a few compounds that show anticancer activity along with antitumor, anti-inflammatory, and analgesic activities [12]. All these sources suggest that choosing a pyridine derivative for our synthesis would be beneficial in terms of cytotoxic effect. This present article is all about the synthesis of metal complex of Schiff base derived from the condensation of 2-pyridylaldehyde (**1**) with (3-dimethylamino)-1-propylamine (**2**). However, the synthesis of the Schiff base ligand *N,N*-dimethyl-*N*-(1-pyridinylmethylidene) propane-1,3-diamine DPMPD (**3**) (**Scheme 1**) has already been reported [13], and previously our group has initially synthesised its corresponding metal complexes [14].



Scheme 1

Experimental

Materials and methods

All the chemicals were purchased from Sigma Aldrich and used without further purification. Other reagents were obtained from commercial sources and used as received. Solvents were purchased from commercial sources and were used for synthesis without further purification while purified and dried solvents were used for spectroscopic measurements.

Synthesis of ligand

The ligand DPMPD (**3**) was prepared by following the process as reported by earlier group of workers [13] and our research group [14]. The liquid product obtained was very dense oily substance which was further used to synthesize metal complex.

Synthesis of metal complex

The metal complex of DPMPD (**3**) (1 mmol) was obtained by adding the metal salt copper perchlorate hexahydrate (1 mmol) to the ligand solution under room temperature (25 °C) and inert condition (**Scheme 2**). The detailed synthesis process has been discussed in the experimental section.

After several trials we were unable to obtain a proper crystalline structure of the complex so to determine the most probable structure of the newly synthesised metal complex CDPMPD (**4**) several spectroscopic tools, such as FT-IR, Mass, UV- Visible along with SEM- EDX and PXRD were utilised.

FT-IR spectroscopy

The FTIR spectra of ligand and its metal complex were obtained on a Bruker alfa 2 apparatus in the range 4000- 400 cm⁻¹. As the complex was solid, so it was examined. as KBr discs [15]. The coordination of azomethine group and formation of metal-N bond were confirmed by shifts analysis in IR spectra.

UV- Visible spectroscopy

The UV-Vis spectra of metal complex (10⁻⁴ mole) were recorded in ACN at room temperature (25 °C). Several absorption bands appear in the spectrum were related to the metal to ligand charge transfer transition and d/d transitions, respectively.

PXRD

Due to the difficulty in obtaining crystalline complex in proper symmetry, X-ray powder diffraction patterns were obtained for the above metal complex. Powder X-ray diffraction spectrum is recorded in Rigaku Japan, Smartlab model X-ray diffractometer equipped with a 3 kW X-ray generator Cu tube, and operable in both Bragg-Brentano and parallel beam geometry. The X-ray powder diffraction patterns were obtained for the metal complex using the X-pert High Score Plus software in the range of 10-40. The experimental result of the powdered complex was quite similar with that of the reference material with JCPDS ID 00-024-1977.

Mass spectra

The mass spectrum of the metal complex exhibits the molecular ion peak at (m/z), which is in agreement with several molecular ion peaks for various fragmentation processes.

SEM- EDX

The SEM data was collected in a JEOL-JSM-IT100 instrument with a smart gold coater and EDX spectrum was collected in an X- Max OXFORD instrument (20 mm²). In EDX spectrum the Cu (II) complex shows C, O, N, and Cl characteristics signals, it clearly confirm the formation of complex CDPMPD, whereas the SEM images clearly indicate that the complex has a crystalline morphology.

In vitro anticancer study

The *in vitro* anticancer study was done upon Hep-G2 cell line which was commercially purchased from National Cell Repository NCCS, Pune, and then cultured in the lab facility for testing. Using seven absorbance

measurements, the percentage growth is calculated at each of the drug concentrations levels. The growth curve of CDPMPD against Hep- G2 cell line exhibited moderate cytotoxic effect [14].

Quantum Chemical Calculations

To ascertain the chemical reactivity of ligand and metal complex DFT analysis has been carried out using Gaussian (G09) software. Using the (UB3LYP) with 6-31G basis set energy of the highest occupied molecular orbital (HOMO), the lowest unoccupied molecular orbital (LUMO), band gap energy, total minimized energy, and dipole moment were calculated. Based on the fact that CDPMPD (**4**) molecule which has shown anticancer activity, we decided to dock this compound into the binding site of topoisomerase II crystal structure (PDB id 4FM9) [16]. The docking result of CDPMPD (**4**) revealed significant affinity of the drug toward the binding site of topoisomerase II.

Results and Discussion

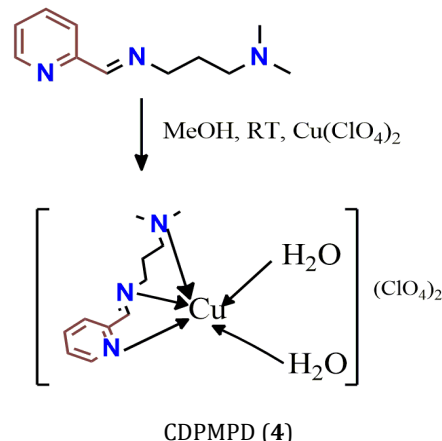
Synthesis of *N,N*-dimethyl-*N*-(1-pyridinylmethylidene) propane-1,3-diamine (DPMPD)

Synthesis of the DPMPD (**3**) was carried out by the condensation of *N,N*-dimethyl-1,3 diaminopropane (**2**) and 2-pyridine carboxaldehyde (**1**) as reported by an earlier group of workers [13]. The liquid product obtained was extracted with DCM and water. Later the solvent was dried over vacuum and a very dense oily substance was used to synthesize the metal complex.

Synthesis of Cu (II) *N,N*-dimethyl-*N*-(1-pyridinylmethylidene) propane-1,3-diamine (CDPMPD)

DPMPD (**3**) (1 mmol) was dissolved in 5 ml of methanol (MeOH) and to the ligand solution, the metal salt copper perchlorate hexahydrate (1 mmol) was added and continued stirring for

about an hour under room temperature and inert condition (**Scheme 2**). The resultant reaction mixture was then kept for evaporation to reduce the volume [17]. Then, on the addition of diethyl ether a dark green colored precipitate was obtained which was further dried and the powdered form of the complex was collected for further characterization.



Scheme 2.

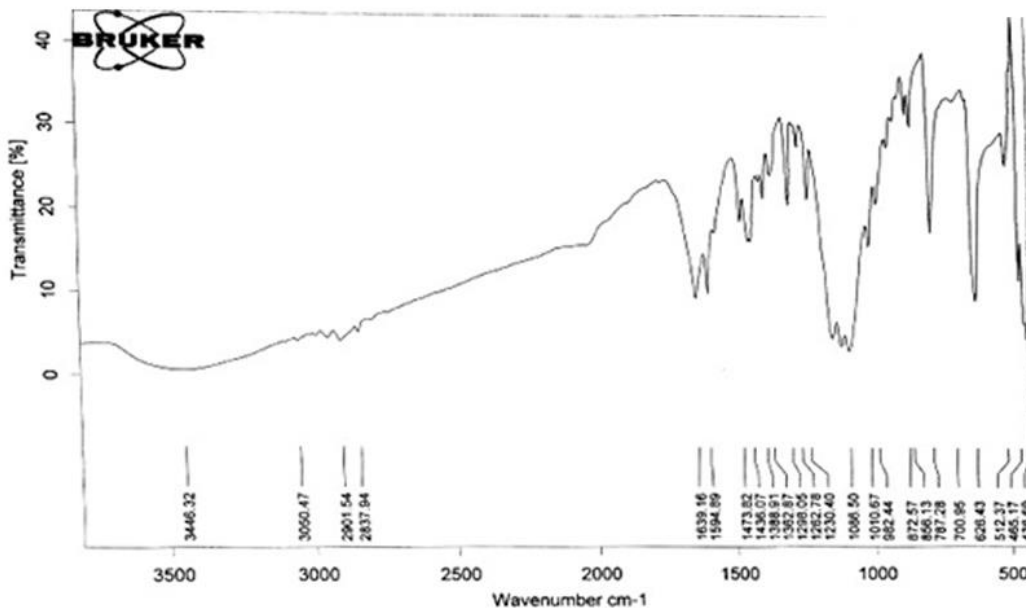
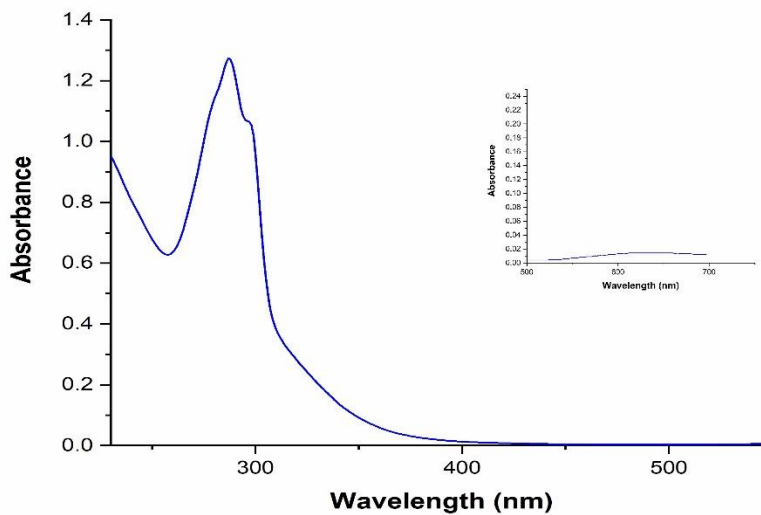
Structural Analysis

IR data analysis

The coordination of the azomethine group to the metal ions was confirmed by a shift in the $\nu(C=N)$ band to a lower frequency by 10 cm⁻¹, as observed in the IR spectra of the complex (**Figure 1**), compared with that in the free ligand band at 1648 cm⁻¹ [18]. The C-H stretch occurring in the 2800-2950 cm⁻¹ region indicating aliphatic chain and in the 3000-3100 cm⁻¹ region for aromatic compound. The band observed near 1588 cm⁻¹ assigned to $\nu(C=C)$. The $\nu(C-N)$ mode occurs near 1388 cm⁻¹, which is almost similar to that found in the free ligand [19,20]. Usually free perchlorate ion appears in between 1094-1100 cm⁻¹ range, which is present in the complex IR spectrum. Another new band observed at 513 cm⁻¹ signifies the formation of Cu-N bond in the complex (**Table 1**).

Table 1. Four main bands appeared in the IR spectra of the complex CDPMPD

Complex	ν (C=N) cm ⁻¹	ν (C-H) cm ⁻¹	ν (C=C) cm ⁻¹	ν (Cu-N) cm ⁻¹
CDPMPD	1648	2800- 2950 3000- 3100	1588	513

**Figure 1.** FT-IR spectrum of CDPMPD complex**Figure 2.** The UV spectra of CDPMPD complex. Inset image shows magnified view of the UV spectrum for d-d transition

UV-Vis data

The UV-Vis spectra of metal complex (10^{-4} mole) were recorded in ACN at room temperature (**Figure 2**). The absorption bands of metal complex appeared at 206 and 286 nm, corresponds to $\pi-\pi^*(-C=C)$ and $n-\pi^*(-C=N)$ transitions, respectively. In addition, the copper complex showed a weak broad band in the regions of 630-700 nm [14, 21] which corresponding to d/d transitions. Complex shows intense bands below 400 nm, which may be attributed to the ligand to metal charge transfer transition.

PXRD analysis

The most useful tool to obtain information regarding the structure of complexes is single-crystal X-ray crystallography. The powder XRD pattern is quite similar for both the observed and calculated values. The diffractogram of Cu (II) complex shows 25 reflections with maxima at $2\theta=19.88$. Reflections were collected in the 2θ range between 3 and 60° with wavelength 1.54 nm (CuK α radiation). The experimental result of the powdered complex

was quite similar with that of the reference material with JCPDS ID 00-024-1977. The size of metal complex was calculated from the observed d_{XRD} patterns using Scherer's formula [22]. The average grain size of metal complex was calculated from this experiment. In the present study, Cu (II) complexes are found to have the grain sizes 711 nm. X-ray diffraction pattern of the CDPMPD complex is depicted in **Figure 3**.

Mass spectra analysis

The intensity of peaks reflects the stability and abundance of the ions [23]. The mass spectrum of the metal complex exhibits the molecular ion peak at (m/z), which is in agreement with the fragment $\{[Cu(DPMPD)(H_2O)_2](ClO_4)+H_2O\}^+$ ion at 408.7, $\{[Cu(DPMPD)(H_2O)_2](ClO_4)+(H_2O)_2\}^+$ at 425.2 and they also exhibit several molecular ion peaks [22] for various fragmentation processes. The observed molecular ion peaks in the mass spectra of the synthesized compounds (**Figure 4**) are in good agreement with their proposed structure arrived from various spectral techniques as well as SEM- EDX and PXRD.

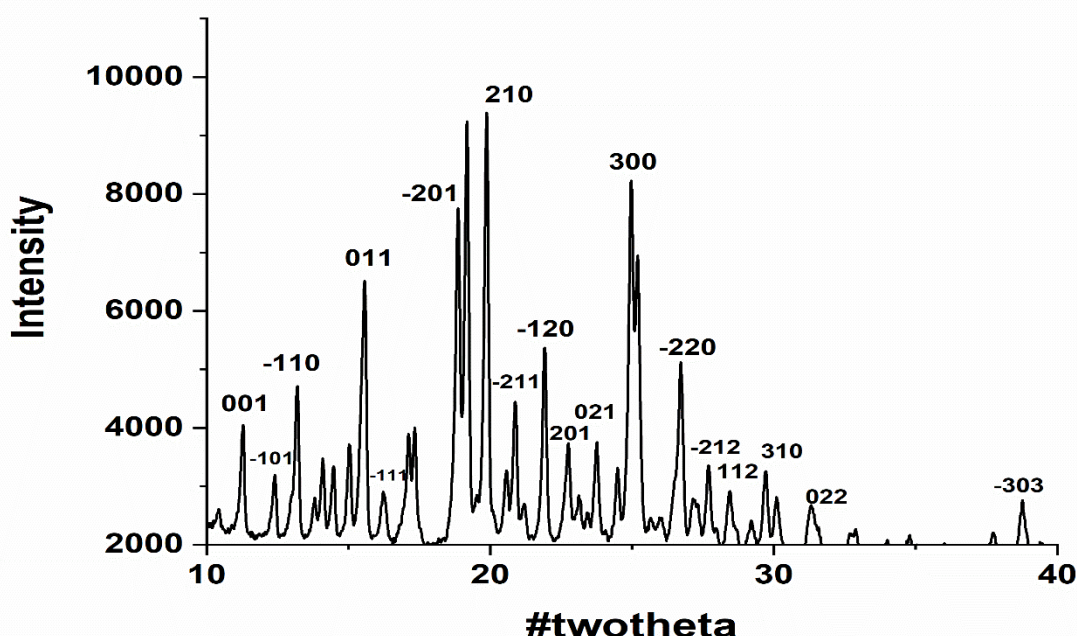
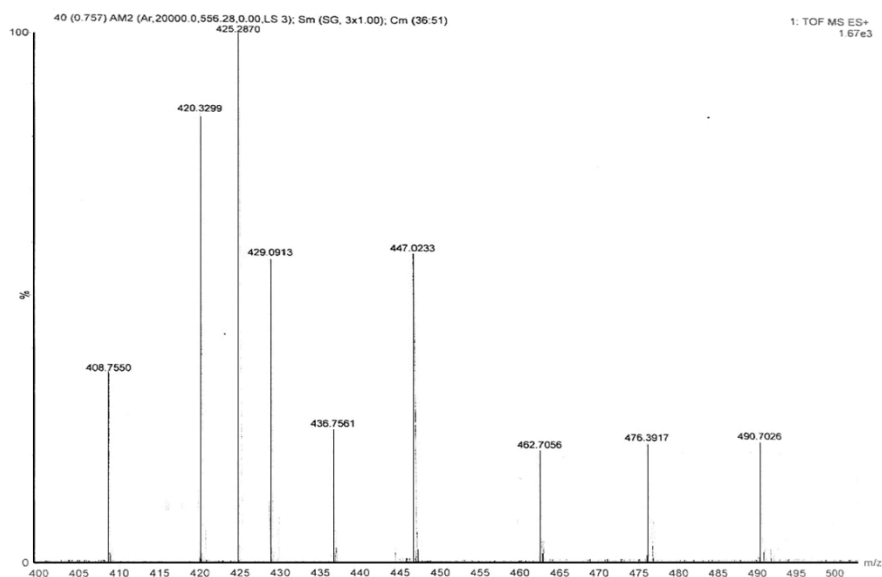


Figure 3. X-ray diffraction pattern of powdered CDPMPD complex has been compared with the reference material with JCPDS ID 00-024-1977 using the X-pert High Score Plus software

**Figure 4.** Mass spectra of CDPMPD

SEM and EDX studies

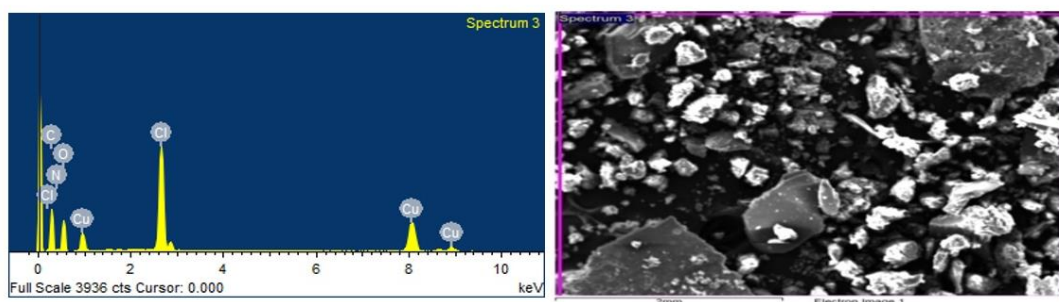
EDX data analysis

The metal complex composition was obtained from Energy Dispersive X-ray (EDX) analysis [24]. In the analysis of Cu (II) complex represented by **Figure 5**, it is observed that experimental atom percentage is close to the expected (theoretical) values. In the EDX spectrum, the Cu (II) complex shows C, O, N, and Cl characteristics signals, it confirms the formation of the complex with the expected

formula. EDX spectrum was collected in an X-Max OXFORD instrument (20 mm^2).

SEM data analysis

The SEM photographs of Cu (II) complex is demonstrated in **Figure 6**. The SEM micrographs show the agglomerate particles of the complex. In the case of the CDPMPD complex, some agglomerates appear to have tiny needles, while the other agglomerates appear to be of plates like morphologies. The SEM images indicate that the complex has a crystalline morphology.

**Figure 5.** EDX images of the CDPMPD complexes

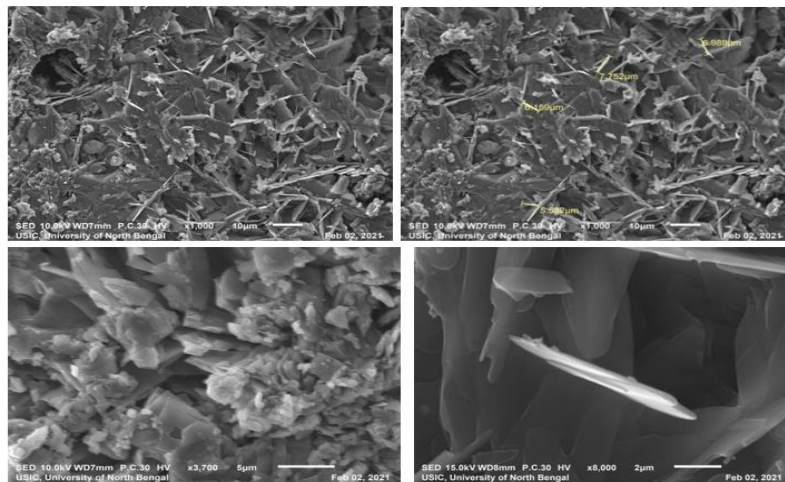


Figure 6. SEM images of the CDPMPD complexes

Anticancer Activity Study

Cell culture and Sulforhodamine B (SRB) assay

Hep-G2 cells were grown in Roswell Park Memorial Institute media (RPMI 1640) containing 10% fetal bovine serum and 2 mM L-glutamine in T-75 flask at 37 °C, 5% CO₂, 95% air and 100% relative humidity for 24 h. After growing, 100 μL cells containing media was inoculated into 96 well plates at a concentration of 5×10³ cells/well. Separately, all the compounds to be tested were solubilised in dimethyl sulfoxide at 100 mg/ml and diluted to 1 mg/ml using water and stored frozen prior to use. Next day, 100 μL of compounds containing media was added in each well (10,

20, 40, and 80 μg/ml) and incubated at standard conditions for 48 h. To terminate the reaction, 50 μL of the cold 30% trichloroacetic acid (TCA) was added and incubated at 4 °C for 1 h. The supernatant was discarded; the plates were washed five times with tap water and air dried. Furthermore, 50 μL of SRB solution at 0.4% (w/v) in 1% acetic acid was added to each well and incubated for 20 minutes at room temperature. After staining, the residual dye was removed by washing five times with 1% acetic acid and the plates were air dried. The bound stain was subsequently eluted with 10 mM trizma base and the absorbance was read on a plate reader at a wavelength of 540 nm with 690 nm reference wavelength (**Figure 7**). The results were obtained in triplicate on

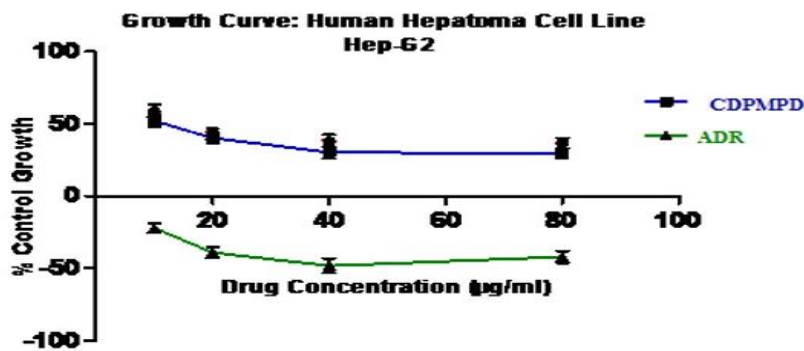


Figure 7. *In vitro* anticancer activity of complex CDPMPD

Table 2. Calculated energy values of CDPMPD using UB3LYP/6-31G basis set

Molecule	E _{HOMO}	E _{LUMO}	ΔE (Band gap)	Energy × 10 ⁻⁴	Dipole Moment
CDPMPD	-2.74 eV	0.14 eV	2.88 eV	-6.08 eV	4.45 D
DPMRD	-5.46 eV	-1.35 eV	4.11 eV	-1.61 eV	1.36 D

separate plates and finally the average values were determined from these three experiments. Using seven absorbance measurements [time zero (Tz), control growth (C), and test growth in the presence of drug at five concentration levels (Ti)], the percentage growth is calculated at each of the drug concentrations levels. Percentage growth inhibition is calculated as: $[(Ti-Tz)/(C-Tz)] \times 100$ for concentrations for which $Ti > Tz$ $[(Ti-Tz)/Tz] \times 100$ for concentrations for which $Ti < Tz$. GI50 was calculated from $[(Ti-Tz)/(C-Tz)] \times 100 = 50$, which is the drug concentration resulting in a 50% reduction in the net protein increase (as measured by SRB staining) in control cells during the drug incubation [14, 25, 26, 27].

Computational Methods

Density functional theory (DFT)

In this study, CDPMPD complex was drawn using Gauss view 5.0 suites. Gaussian (G09) [28] software was used to optimize the chemical structure for this molecule. DFT model of unrestricted Becke's three parameters exchange potential and Lee-Yang-Parr correlation functional method (UB3LYP) with

6-31G basis set [29, 30] was applied for completing the minimum energy search. Energy of the highest occupied molecular orbital (HOMO), the lowest unoccupied molecular orbital (LUMO), band gap energy, total minimized energy, and dipole moment of the complex and ligand are shown in **Table 2** [31].

Molecular docking method

In this study, the target receptor i.e. 3D X-ray crystal structure of topoisomerase II (PDB ID: 4FM9) was extracted from Research Collaboratory for Structural Bioinformatics-Protein Data Bank (RCSB - PDB) (<http://www.rcsb.org/>). All bound waters, ligands, and cofactors were removed from this crystal structure prior to docking [31, 32], using Molegro Molecular Viewer (MMV) 2.5.0 suite (CLC Bio, Qiagen Inc.). Auto Dock 4.2 (AD 4.2) [21] software under Auto Dock Tools-1.5.6 (ADT) was used to generate best binding poses for this ligand. The receptor molecule was prepared by adding all hydrogen with no bond order using graphical user interface of ADT. CDPMPD molecule as ligand was further prepared as PDB format from the optimized

Table 3. Binding energy and Van der Waals interactions of ligand CDPMPD into topoisomerase II receptor

Compound	PDB ID	Binding Energy (kcal/mol)	van der Waals interactions
CDPMPD	4FM9	-5.94	PRO593, SER591, LEU592, TYR590, ILE577, GLN542, ASP543, LYS550, GLN544, TYR686, SER547, LYS701, ASP683, and TYR684.

Gaussian (G09) output to assist rigid docking using Avogadro suite [33]. Active torsions have been assigned to maximum number of atoms. Kollman charges were applied to the protein.

The ligand and protein molecule were converted into their proper readable format (pdbqt). The size of grid box was fixed at size of dimension $90 \times 90 \times 90 \text{ \AA}$. Similarly the x, y, and z coordinates of the grid box were set at 32.645, 39.86, and 14.468 with overall spacing of 0.9 \AA . In general, all other docking parameters were kept as default. The best docked model with higher negative binding energy was converted into pdb format from dlg output and considered for further studies. This output file (protein-ligand complex) was analysed using Discovery Studio Visualizer (v20.1.0.19295) (**Table 3**).

Frontier molecular orbitals (FMOs) analysis

FMOs theory is one of the best ways for explaining the chemical stability of a compound using HOMO (the highest occupied molecular orbital) and LUMO (the lowest unoccupied molecular orbital) energies [31, 34]. Here, energy of HOMO and LUMO were computed using DFT-UB3LYP/6-31G method. HOMO has ability to donate electron, behave like nucleophile and, on the other hand, LUMO has electron accepting tendency from nucleophile (act as electrophile) [35]. The band gap energy of HOMO and LUMO (ΔE_{HL}) has given information about chemical reactivity as well as

kinetic stability of a molecule. A molecule with large ΔE_{HL} is described as hard molecule with less or much less polarizability. Similarly, soft systems (small ΔE_{HL}) have high chemical reactivity, and polarizability [36, 37]. Besides, molecules possessing higher values of dipole moment have a tendency to take part in strong intermolecular interaction. In this study, CDPMPD molecule has displayed lower ΔE_{HL} value of 2.88 eV (**Figure 8b**) as compared to DPMPD (4.11 eV). Hence, the CDPMPD is considered as the soft molecule with polarizable and reactive chemical species. It is also found that it has profound dipole moment of the value of 4.45 D compared to DPMPD (1.36 D).

Molecular docking study

Based on the fact that CDPMPD molecule which has shown anticancer activity, we decided to dock this compound into the binding site of topoisomerase II crystal structure (PDB id 4FM9). The docking result of CDPMPD (**Figure 9**) revealed significant affinity of the drug toward the binding site of topoisomerase II. The drug is nicely fitted into the active site of the receptor and showing binding energy of -5.94 kcal/mol and forming one π -donor hydrogen bond with residue LEU685 at the binding site. Two π -alkyl interactions are found between the CDPMPD molecule and amino acid residue

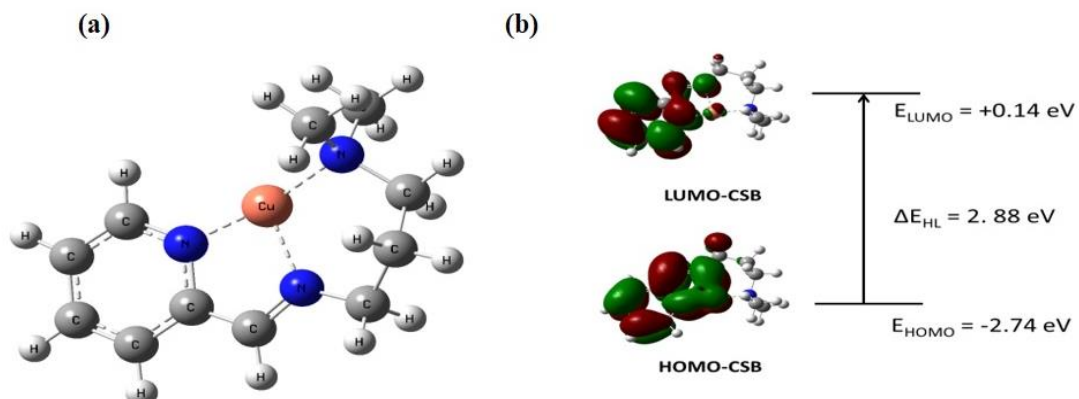


Figure 8. CDPMPD molecule having (a) optimized chemical structure and (b) HOMO-LUMO orbitals

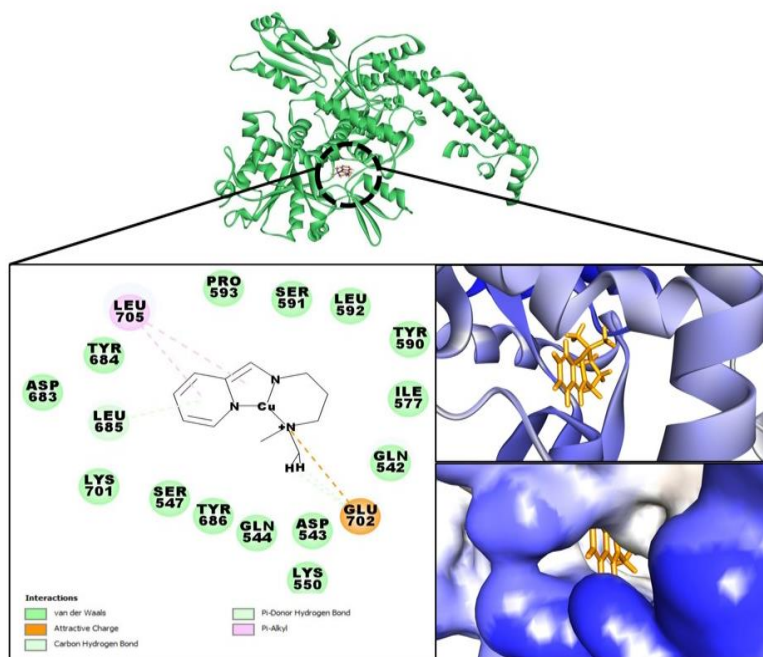


Figure 9. Molecular docking interaction of CDPMPD with topoisomerase II (PDB ID: 4FM9)

LEU705. Likewise, it has shown Van der Waals interactions with PRO593, SER591, LEU592, TYR590, ILE577, GLN542, ASP543, LYS550, GLN544, TYR686, SER547, LYS701, ASP683, and TYR684 residues of the receptor [16,31].

Conclusion

N,N-dimethyl-*N*-(1-pyridinylmethylidene) propane-1,3-diamine (DPMPD) has been synthesised and its metal salt copper (*N,N*-dimethyl-*N*-(1 pyridinylmethylidene)propane-1,3-diamine) perchlorate (CDPMPD) obtained by the addition of Cu(ClO₄)₂•6 H₂O and collected in the form of fine powder. Both the ligand and the metal complex were characterized using different spectroscopic techniques. The grain size of the metal complexes was estimated by the Scherrer Formula using powder XRD. The experimental results of the powdered complex were quite similar to that of the reference material with JCPDS ID 00-024-1977. *In vitro* anticancer study of the complex exhibited the moderate cytotoxic effect in the Hep-G2 cell line and the molecular docking study was performed with topoisomerase II (PDB ID: 4FM9) receptor. DFT

analysis has been carried out to ascertain the chemical reactivity of the compound.

Orcids

Rajesh Kumar Das

<https://orcid.org/0000-0001-9433-4711>

Deboshmita Mukherjee

<https://orcid.org/0000-0001-5062-1399>

Sahin Reja

<https://orcid.org/0000-0002-9659-9016>

Kaushik Sarkar

<https://orcid.org/0000-0002-3782-0948>

Ambica Kejriwal

<https://orcid.org/0000-0002-6361-5075>

Acknowledgements

The authors are grateful to the Departmental Special Assistance Scheme under the University

Grants Commission, New Delhi and Head, all the members, Department of Chemistry, University of North Bengal, Darjeeling, India, for providing various facilities in connection with this research work. RKD is grateful to University Grants Commission, New Delhi, for the project F.30-515/2020(BSR), 12.02.2020, F.D. Diary No. 9719, 23.01.2020.

References

- [1]. M.F Jones., S.M. Roberts, *J. Chem. Soc., Perkin Trans. 1*, **1988**, 2927-2932. [[Crossref](#)], [[Google Scholar](#)], [[Publisher](#)]
- [2]. G.B. Elion, *Angew. Chem. Int. Ed. Eng.*, **1989**, 28, 870-878. [[Crossref](#)], [[Google Scholar](#)], [[Publisher](#)]
- [3]. P. Arora, V. Arora , H.S. Lamba, D. Wadhwa, *IJPSC*; **2012**, 3, 2947-2954. [[Google Scholar](#)], [[Publisher](#)]
- [4]. A. Czarnik, *Acc. Chem. Res.*, **1996**, 29, 112-113. [[Crossref](#)], [[Google Scholar](#)], [[Publisher](#)]
- [5]. A.P. Kozikowski, Comprehensive Heterocyclic Chemistry, Pergamon Press, **1984**, Oxford, New York. [[Google Scholar](#)], [[Publisher](#)]
- [6]. E. Vitaku; T.D. Smith; T.J. Njardarson, *J. Med. Chem.*, **2014**, 57, 10257-10274. [[Crossref](#)], [[Google Scholar](#)], [[Publisher](#)]
- [7]. A.A. Altaf, A. Shahzad, Z. Gul, N. Rasool, A. Badshah, B. Lal, E. Khan, *J. drug des. med. chem.*, **2015**; 1, 1-11. [[Crossref](#)], [[Google Scholar](#)], [[Publisher](#)]
- [8]. E. Lukevits, L. Demicheva, *Chem. Heterocycl. Compd.*, **1993**, 29, 243-267. [[Crossref](#)], [[Google Scholar](#)], [[Publisher](#)]
- [9]. W.B. Zhang, X.T. Yang, J.B. Ma, Z.M. Su, S.L. Shi, *J. Am. Chem. Soc.* **2019**, 141, 5628-5634. [[Crossref](#)], [[Google Scholar](#)], [[Publisher](#)]
- [10]. Y. Thigulla, T.U. Kumar, P. Trivedi, B. Ghosh, *Chem. Sel.*, **2017**, 7, 2718-2721. [[Crossref](#)], [[Google Scholar](#)], [[Publisher](#)]
- [11]. H.A. Abadi, M.T. Ibrahim, M.K. Abouzid, J. Lehmann, N.H. Tinsley, D.B. Gary, A.G. Piazza, *Bioorg. Med. Chem.*, **2009**, 17, 5974-5982. [[Crossref](#)], [[Google Scholar](#)], [[Publisher](#)]
- [12]. M.H. Helal, S.A. El-Awdan, M.A. Salem, A.T. Abd-elaziz, Y.A. Moahamed, A.A. El-Sherif, A.G.M. Mohamed, *Spectrochim. Acta A Mol. Biomol. Spectrosc.*, **2015**, 135, 764-773. [[Crossref](#)], [[Google Scholar](#)], [[Publisher](#)]
- [13]. S. Chopra, J. Singh, N. Singh, N. Kaur, *Anal. Methods*, **2014**, 6, 9030-9036. [[Crossref](#)], [[Google Scholar](#)], [[Publisher](#)]
- [14]. D. Mukherjee, S. Reja, K. Sarkar, T.K. Fayaz, P. Kumar, A. Kejriwal, P. Das, P. Sanphui, R.K. Das, *Inorg. Chem. Commun.*, **2022**, 146, 110190. [[Crossref](#)], [[Google Scholar](#)], [[Publisher](#)]
- [15]. P. Gull, A.A. Hashmi, *J. Mol. Struct.*, **2017**, 1139, 264-268. [[Crossref](#)], [[Google Scholar](#)], [[Publisher](#)]
- [16]. A.F. Eweas, N.M. Khalifa, N.S. Ismail, M.A. Al-Omar, A.M.M. Soliman, *Med. Chem. Res.*, **2014**, 23, 76-86. [[Crossref](#)], [[Google Scholar](#)], [[Publisher](#)]
- [17]. N. Mohan, S.S. Sreejith, M.R. Prathapachandra Kurup, *Polyhedron*, **2019**, 173, 114129. [[Crossref](#)], [[Google Scholar](#)], [[Publisher](#)]
- [18]. M.M. Elsayy, A.A. Faheim, S.S. Salem, M.E. Owda, Z.H. Abd El-Wahab, H.A. El-Wahab, *Appl. Organomet. Chem.*, **2021**, 35, e6196. [[Crossref](#)], [[Google Scholar](#)], [[Publisher](#)]
- [19]. S. Seth, A.K. Das, T.C.W. Mak, *Acta Cryst.*, **1995**, C51, 2529-2532. [[Crossref](#)], [[Google Scholar](#)], [[Publisher](#)]
- [20]. C. Justin Dhanaraj, J. Johnson, *J. Therm. Anal. Calorim.*, **2016**, 127, 1845-1862. [[Crossref](#)], [[Google Scholar](#)], [[Publisher](#)]
- [21]. A. Ambala, Ch.A. Lincoln, *Chem. Data Collect.*, **2020**, 27, 100372. [[Crossref](#)], [[Google Scholar](#)], [[Publisher](#)]
- [22]. J.D. Chellaian, S. Raj S.S., *J. Heterocycl. Chem.*, **2021**, 58, 928-941. [[Crossref](#)], [[Google Scholar](#)], [[Publisher](#)]
- [23]. P. Talukder, A. Datta, S. Mitra, G. Rosari, *Z Naturforsch. B*, **2004**, 59b, 655-660. [[Crossref](#)], [[Google Scholar](#)], [[Publisher](#)]
- [24]. A. Ambala, Ch.A. Lincoln, *Int. J. Chemtech Res.*, **2020**, 13, 29-37. [[Crossref](#)], [[Publisher](#)]
- [25]. A. Allahresani, F. Ghorbanian, M.A. Nasseri, M. Kazemnejadi, *J. Appl. Organomet. Chem.*, **2022**, 2, 39-54. [[Crossref](#)], [[Google Scholar](#)], [[Publisher](#)]
- [26]. S. Reja, D. Mukherjee, P. Das, P. Kumar, R. Kumar Das, *J. Mol. Struct.*, **2021**, 1245, 131006. [[Crossref](#)], [[Google Scholar](#)], [[Publisher](#)]
- [27]. P. Kumar, A.K. Singh, V. Raj, A. Rai, A.K. Keshari, D. Kumar, B. Maity, A. Prakash, S. Maiti,

- S. Saha, *Int. J. Nanomedicine*, **2018**, *13*, 975-990. [[Crossref](#)], [[Google Scholar](#)], [[Publisher](#)]
- [28]. T.J. M.Frisch *et al.*, Gaussian 09, Revision E.01. Gaussian, Inc., Wallingford CT, **2009**. [[Google Scholar](#)], [[Publisher](#)]
- [29]. J.P. Stephens, F.J. Devlin, C.F. Chabalowski, M.J. Frisch, *J. Phys. Chem.*, **1994**, *98*, 11623-11627. [[Crossref](#)], [[Google Scholar](#)], [[Publisher](#)]
- [30]. C. Lee, W. Yang, R.G. Parr, *Physical review B*, **1988**, *37*, 785. [[Crossref](#)], [[Google Scholar](#)], [[Publisher](#)]
- [31]. K. Sarkar, R. Kumar Das, *J. Comput. Biophys. Chem.*, **2021**, *20*, 641-654. [[Crossref](#)], [[Google Scholar](#)], [[Publisher](#)]
- [32]. M.G. Morris, R. Huey, W. Lindstrom, F.M. Sanner, K.R. Belew, S.D. Goodsell, J.A. Olson, *J. Comput. Chem.*, **2009**, *16*, 2785-2791. [[Crossref](#)], [[Google Scholar](#)], [[Publisher](#)]
- [33]. D.M. Hanwell, D.E. Curtis, D.C. Lonie, T. Vandermeersch, E. Zurek, G.R. Hutchison, *J. Cheminform*, **2012**, *4*, 1758-2946. [[Crossref](#)], [[Google Scholar](#)], [[Publisher](#)]
- [34]. Y. Umar, S. Abdalla, *J. Solution Chem.*, **2017**, *46*, 741-758. [[Crossref](#)], [[Google Scholar](#)], [[Publisher](#)]
- [35]. L.J. Reed, *J. Phys. Chem. A*, **1997**, *101*, 7396-7400. [[Crossref](#)], [[Google Scholar](#)], [[Publisher](#)]
- [36]. V. Arjunan, L. Devi, R. Subbalakshmi, T. Rani, S. Mohan, *Spectrochim. Acta A Mol. Biomol. Spectrosc.*, **2014**, *130*, 164-177. [[Crossref](#)], [[Google Scholar](#)], [[Publisher](#)]
- [37]. O. El-Gammal, T. Rakha, H. Metwally, G.A. El-Reash, *Spectrochim. Acta A Mol. Biomol. Spectrosc.*, **2014**, *127*, 144-156. [[Crossref](#)], [[Google Scholar](#)], [[Publisher](#)]